JPn

Neuroscience

The Journal of Physiology

Suprachiasmatic nucleus function and circadian entrainment are modulated by G protein-coupled inwardly rectifying (GIRK) channels

L. M. Hablitz, H. E. Molzof, J. R. Paul, R. L. Johnson and K. L. Gamble

Department of Psychiatry and Behavioral Neurobiology, University of Alabama at Birmingham, Birmingham, AL 35294, USA

Key points

- Many time-of-day cues are mediated by G protein-coupled signals within the clock centre (the suprachiasmatic nucleus, SCN) of the mammalian brain.
- The role of G protein-coupled inwardly rectifying potassium (GIRK) channels in SCN function and entrainment has yet to be determined.
- GIRK channels are necessary for proper day-time SCN neuronal resting membrane potential, neuropeptide Y signalling, and re-entrainment to phase advances of the light–dark (LD) cycle.
- GIRK channel activation is sufficient to mimic non-photic phase shifts of the molecular clock.
- GIRK channels act as an essential part of the non-photic entrainment system, and could play a critical role in diseases such as epilepsy or addiction that have strong circadian comorbidities.

Abstract G protein signalling within the central circadian oscillator, the suprachiasmatic nucleus (SCN), is essential for conveying time-of-day information. We sought to determine whether G protein-coupled inwardly rectifying potassium channels (GIRKs) modulate SCN physiology and circadian behaviour. We show that GIRK current and GIRK2 protein expression are greater during the day. Pharmacological inhibition of GIRKs and genetic loss of GIRK2 depolarized the day-time resting membrane potential of SCN neurons compared to controls. Behaviourally, GIRK2 knockout (KO) mice failed to shorten free running period in response to wheel access in constant darkness and entrained more rapidly to a 6 h advance of a 12 h:12 h light–dark (LD) cycle than wild-type (WT) littermate controls. We next examined whether these effects were due to disrupted signalling of neuropeptide Y (NPY), which is known to mediate non-photic phase shifts, attenuate photic phase shifts and activate GIRKs. Indeed, GIRK2 KO SCN slices had significantly fewer silent cells in response to NPY, likely contributing to the absence of NPY-induced phase advances of PER2::LUC rhythms in organotypic SCN cultures from GIRK2 KO mice. Finally, GIRK channel activation is sufficient to cause a non-photic-like phase advance of PER2::LUC rhythms on a *Per2^{Luc+/−}* background. These results suggest that rhythmic regulation of GIRK2 protein and channel function in the SCN contributes to day-time resting membrane potential, providing a mechanism for the fine tuning responses to non-photic and photic stimuli. Further investigation could provide insight into disorders with circadian disruption comorbidities such as epilepsy and addiction, in which GIRK channels have been implicated.

Abbreviations CNQX, 6-cyano-7-nitroquinoxaline-2,3-dione; CT, circadian time; D-AP5, D-(−)-2-amino-5-phosphonopentanoic acid; DD, constant darkness; GIRK, G protein-coupled inwardly rectifying potassium channel; KO, knockout; LD, light–dark (cycle); LUC, luciferase; NPY, neuropeptide Y; Per2, Period 2; SCN, suprachiasmatic nucleus; TPQ, tertiapin-q; WT, wild type; ZT, zeitgeber time.

Introduction

The central circadian oscillator in the suprachiasmatic nucleus (SCN) of the hypothalamus contains ~20,000 coupled neurons (Welsh *et al.* 2010). A transcription–translation feedback loop called the 'molecular clock' drives rhythmic gene expression in individual SCN neurons and regulates daily oscillations in action potential firing and excitability, with increased neuronal firing during the day and relative quiescence during the night (Kuhlman & McMahon, 2006). This day–night variation in electrical output from the SCN drives circadian rhythms in other brain areas and the body. The timing of these molecular and neurophysiological rhythms can be altered by environmental cues including photic (light) and non-photic (stress, exercise, etc.) stimuli (Albrecht, 2012). These alterations or phase shifts occur daily, entraining the animal to its environment. Although much is known about the neurotransmitter systems that underlie these entraining pathways, the molecular mechanisms that couple receptor activation to the changes in SCN neuronal output that ultimately shift circadian phase and drive entrainment are not fully understood.

One mediator of intracellular phase shifting signals is G protein signalling, and many of these second messenger pathways are critical for maintaining SCN rhythmicity and enabling photic and non-photic entrainment (Cheng *et al.* 2004; Aton *et al.* 2006; Dahdal *et al.* 2010; Doi *et al.* 2011; Brancaccio *et al.* 2013). We hypothesize that this abundance of crucial G protein signalling in SCN neurons may activate G protein-coupled inwardly rectifying potassium (GIRK) channels, which have been implicated in diseases such as epilepsy and addiction (Hibino *et al.* 2010; Luscher & Slesinger, 2010). Furthermore, GIRK channel activation within the SCN may alter neurophysiological function and the ability of environmental stimuli to reset circadian clock phase. We use a variety of electrophysiological, behavioural, and molecular assays to determine: when GIRK channel protein levels and activation are highest within the SCN, the effect of GIRK channel activation on SCN neuronal function, and the necessity of GIRK channels for circadian entrainment.

Methods

Ethical approval

All animal care, handling, and housing were in compliance with the University of Alabama at Birmingham's Institutional Animal Care and Use Committee guidelines.

Animals and housing

All mice in these experiments were 2–4 months of age to reduce developmental or ageing phenotypes (Turek *et al.*

1995; Biello, 2009). Only male mice were used for Western blotting and behavioural experiments (Ruiz de Elvira *et al.* 1992; Vyazovskiy *et al.* 2006). Three separate mouse lines were used: (1) C57/BL/6 mice (Western blotting experiments); (2) GIRK2 knockout animals on a C57/BL6 background (Signorini *et al.* 1997) (electrophysiology and circadian behaviour); and (3) *Per2^{Luc+/−}* mice (Yoo *et al.* 2004) on a C57/BL6 background crossed with the GIRK2 line for at least two generations before use in experiments (bioluminescence assays of molecular clock function). Separate cohorts of mice were used for each different type of experiment.

Western blotting

For light–dark (LD) experiments (Fig. 1*A* and *B*), mice were group-housed with food and water *ad libitum* in a 12 h:12 h LD cycle. Mice were killed every 4 h over a 24 h period (Zeitgeber time 0 or ZT 0, defined as lights on). For constant darkness (DD) experiments (Fig. 1*C* and *D*), mice were single-housed on running wheels in DD for 2 weeks. Animals were killed during either the subjective day at circadian time 4 (CT 4; CT 12 defined activity onset) or subjective night (CT 16). Activity onset was predicted using linear regression analysis for the preceding seven activity onsets. For all experiments during the dark, mice were killed by cervical dislocation followed by enucleation with the aid of night vision goggles in order to prevent photic signalling during brain extraction. Hypothalamic slices (600 μm) were prepared using a vibroslicer (7000 smz, Campden Instruments Ltd, Lafayette, IN, USA), followed by dissection of the SCN under a Zeiss dissection microscope. Protein lysates were prepared, and immunoblotting for GIRK1 (1:500, Alamone Labs, Israel) and GIRK2 (1:750, Millipore, MA, USA) was performed by loading 10 μg of protein per sample as analysed by a BCA protein assay. Previous studies have shown that GIRK1 and GIRK2 both exhibit multiple bands in Western blots within the brain. For GIRK1, the three bands indicate different glycosylation states (Koyrakh *et al.* 2005; Aguado *et al.* 2008). GIRK2 exhibits multiple splice variants (Lesage *et al.* 1995; Koyrakh *et al.* 2005; Aguado *et al.* 2008). For densitometry analysis, all bands for each protein were quantified together for assessment of total protein levels, and the uppermost heavily glycosylated band of GIRK1 (75 kDa, Fig. 1) was analysed for rhythmicity of GIRK1 glycosylation. For the LD analysis, each blot was normalized to the mean ZT 5 time point as a positive control. β-Actin (1:40,000, Millipore, MA, USA) was used as a loading control.

Electrophysiology

Mice were killed either at ZT 2 or ZT 10.5 (day and night recordings, respectively) by cervical dislocation. For

whole-cell electrophysiology, all recordings were made between projected ZT 3–9 (day) or ZT 12–17 (night). For loose-patch electrophysiology, all recordings were made between projected ZT 4–6 in the presence of 2.35 μM NPY (American Peptide, Sunnyvale, CA, USA) or vehicle (water). Brains were harvested, sectioned at 200 μm on a vibroslicer (7000 smz, Campden Instruments Ltd), and transferred to an open recording chamber (Warner Instruments, Hamden, CT , USA) that was continuously perfused at a rate of 2.0 ml min^{-1} with extracellular solution consisting of (in mM) NaCl 124, NaHCO$_3$ 20, Na$_2$HPO$_4$ 1, MgSO$_4$ 1.3, glucose 10, KCl 3.5, CaCl$_2$ 2.5 (added the day of the experiment), with osmolality adjusted to 300–305 mosmol kg^{-1}), bubbled with 5% CO$_2$–95% O$_2$, and heated to 34 $\pm$ 0.5°C. Neurons were visualized with an Olympus BX51WI (Olympus America Inc., Center Valley, PA, USA) using infrared-differential interference contrast optics. Electrodes with a pipette resistance of ~4–6 MΩ were filled with filtered, potassium gluconate solution consisting of (in mM): potassium gluconate 135, KCl 10, Hepes 10, EGTA 0.5, then adjusted to pH 7.4 with KOH (as in Kuhlman & McMahon, 2004). Electrophysiological signals were processed and controlled by a Multiclamp 700B amplifier, and pClamp 10.02 software (Axon Instruments, Union City, CA, USA). Recordings were sampled at 20 kHz and filtered at 10 kHz. In order to block synaptic transmission (as in Fig. 2): bicuculline (30 μM) and CdCl$_2$ (200 μM) (Sigma-Aldrich, St Louis, MO, USA), D-AP5 (50 μM) and CNQX (10 μM) (Abcam, Cambrige, MA, USA), and TTX (1 μM) (Tocris Biosciences, Minneapolis, MN, USA) were added to the bath solution. To isolate GIRK currents (Fig. 2) the concentration of KCl was increased from 3.5 mM to 30 mM in order to increase potassium conductance across the membrane (refer to Fu *et al.* 2004). The GIRK channel antagonist Tertiapin-Q (0.2 μM; Alamone Labs) was used for experiments in Fig. 3. Input resistance and resting membrane potential were calculated as specified in Kuhlman *et al.* (2003). Resting membrane potential, action potential amplitude, and firing rate were calculated from 30 s gap-free current-clamp recordings. All cells included in these analyses required, in voltage-clamp mode, ≤35 pA holding current in order to clamp membrane potential at −65 mV and an action potential amplitude of greater than 10 pA during the current-clamp step protocol. All data were collected within 6 min of membrane rupture to minimize any potential washout effects from the whole-cell recording (Schaap *et al.* 1999). Loose patch recordings were obtained in gap-free mode with an average seal resistance of 39 MΩ. Average spike rate was calculated from at least 1 min of the 2 min trace. Induced currents for ML297 and NPY application were determined by holding the cell at −80 mV in gap-free voltage-clamp mode in a high potassium (30 mM) solution (as in Hamasaki *et al.* 2013). Either ML297 (10 μM) or NPY (2.35 μM) were both applied for at least 1 min. The change in current following drug application was compared to that of high potassium alone within the same cell. For all electrophysiological experiments, at least three biological replicates with at least four cells per animal were used, unless otherwise indicated. There was no specific regional bias when recording within the SCN.

Behavioural analysis

All mice were housed in individual wheel cages. Wheel-running activity or general cage activity (via infrared motion-sensors from Spy Town, Melville, NY, USA; as in Fig. 4*A* and *B*) was recorded and analysed using Clocklab software (Actimetrics, Wilmette, IL, USA). For behavioural analysis, one WT animal was excluded due to low activity/equipment failure. Free-running period was measured by χ^2 periodogram analysis of 7–10 days in constant dark conditions (Fig. 4). One KO mouse (out of 8) had a free running period of 23.3 h, which was 6.5 SDs from the mean and was therefore excluded from behavioral analysis. Activity profiles from mice housed on wheels in constant darkness were acquired using Clocklab software. Each profile was aligned to CT 12, activity onset. Then, the average counts of WT and KO mice during the subjective day and subjective night were compared. Entrainment was defined as the first day when both the activity onset and alpha length (activity period) were within 20 min of those predicted 4 days prior to the light change. Clocklab software was used to determine activity onset. Offset was defined as the last activity bout where three out of six of the previous bouts were above 3 revolutions per minute. Alpha length was calculated by subtracting onset time from offset time.

Bioluminescence assays

Organotypic SCN cultures from GIRK2 KO or WT *Per2*$^{Luc+/-}$ mice were prepared and treated within the first 7 days for 1 h beginning at CT 3–5 (where CT 12 is defined as peak bioluminescence, drug timing specified for each experiment) with 2.35 μM NPY (American Peptide), 10 μM ML297 (Days *et al.* 2010) or vehicle (either water or 0.02% DMSO, respectively), using identical culture media and methods described in Besing *et al.* (2012). Data were acquired and analysed with Lumicycle Analysis software (Actimetrics, Inc, Wilmette, IL, USA), and recordings with a goodness of fit greater than 85% were used for analysis. Phase shifts were calculated by comparing two predictions for the time of the first peak post treatment: one prediction determined from at least three cycles before treatment and a second prediction determined from at least three cycles after treatment. The difference between these two predictions indicated the size of the phase shift.

Statistical analysis

All statistical analysis was performed with PASW Statistics 18. GIRK channel protein expression was analysed for rhythmicity using a cosinor analysis (as in Bray *et al.* 2013). For comparisons of means, an independent samples *t* test or ANOVA was used for comparisons between two means or two or more means, respectively. Two factor designs were analysed with a two-way ANOVA with repeated measures when appropriate. In cases of a non-normal distribution, a non-parametric Kruskal–Wallis test was used followed by median test *post hoc* analyses. Finally, to assess whether the number of silent cells changed in response to NPY treatment, a G likelihood-ratio test was used. *Post hoc* analyses employed a Fisher's exact test, with a Bonferroni-corrected α of 0.025. For all other tests, significance was ascribed at $P < 0.05$.

Results

GIRK channel protein and function is regulated in a circadian manner within the SCN, influencing day-time neurophysiology

To determine if GIRK1 and GIRK2 channel subunits were present within the SCN, and if levels of these proteins changed over the course of the day, we analysed SCN samples from mice at 4 h time points across a 12 h:12 h light–dark (LD) cycle. Using Western blot analysis, GIRK1 and GIRK2 protein was present within the SCN, and GIRK2 (but not GIRK1) expression patterns significantly fitted a 24 h rhythm (cosinor analysis; GIRK1: $R^2 = 0.114$,

$P > 0.05$; GIRK2: $R^2 = 0.184$, $P < 0.05$; $n = 3$–6 per time point) with peak GIRK2 protein levels occurring at ZT 6.47 ± 0.3 h (amplitude, -0.25 ± 0.1; mesor, 0.59 ± 0.1; Fig. 1*A* and *B*). Because GIRK1 shows variation in the heavily glycosylated state, the glycosylated state was analysed for rhythmicity and showed diurnal variation but failed to reach statistical significance ($R^2 = 0.195$, $P = 0.06$). Although GIRK2 expression exhibited a 24 h rhythm in LD, it was necessary to examine protein levels in the SCN from animals housed in constant darkness (DD) to assess whether this rhythm was endogenously generated rather than driven by the light cycle. GIRK2 protein expression from animals housed for at least 14 days in DD had significantly higher protein levels during the subjective day (CT 4 based on activity onset) compared to night (CT 16; independent samples *t* test, $t_{(5)} = 2.83$, $P < 0.05$; $n = 3$–4 per time point). As expected, levels of both the heavily glycosylated form and total GIRK1 did not vary between time points (Fig. 1*C* and *D*).

In order to determine whether higher levels of GIRK2 protein during the day could contribute to a change in basal GIRK activation over the course of the day, we used whole-cell, voltage-clamp electrophysiology and pharmacological inhibition of synaptic transmission (1 μM TTX, 30 μM bicuculline, 50 μM D-AP5, 10 μM CNQX, and 200 μM CdCl$_2$) along with increased KCl (30 mM) for increased potassium conductance, in order to isolate currents from SCN neurons from wild-type and GIRK2 knockout animals in response to a slow ramp (2.5 s) from -140 mV to -20 mV. Peak inward current was significantly greater during the day in WT neurons
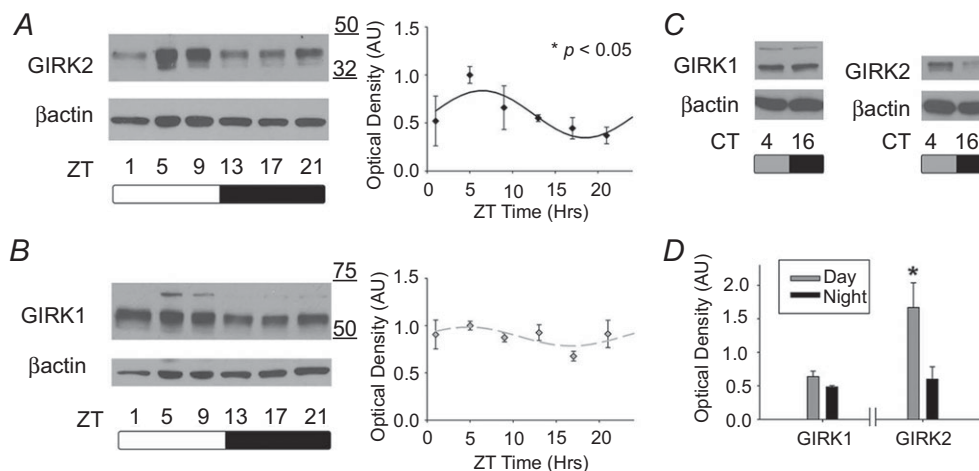

Figure 1. GIRK2, but not GIRK1, protein levels are regulated in a circadian manner
A, representative immunoblots for GIRK2 from mouse SCN out of an LD cycle (left). Relative optical density (mean ± SEM) for GIRK2 throughout the day with lines indicating the predicted cosinor curve (*$P < 0.05$, right). $n = 5$–6 per time point. *B*, representative immunoblot for GIRK1 in mouse SCN across an LD cycle (left). Relative optical density (mean ± SEM) for GIRK1 at each time point throughout the day with predicted cosinor curve (right). $n = 3$–5 per time point. *C*, representative GIRK1 (left) and GIRK2 (right) blots from mouse SCN out of DD at CT 4 (subjective day) and CT 16 (subjective night). *D*, relative optical density (mean ± SEM) between subjective day and night for GIRK1 and GIRK2. *$P < 0.05$, $n = 3$–4 per time point.

(-88.1 ± 5.7 pA) compared to night (-61.3 ± 4.6 pA), and this difference was not seen in KO neurons (day: -64.4 ± 5.4 pA; night: -67.9 ± 6.3 pA; two-way ANOVA, genotype by time interaction: $F_{(1,122)} = 6.53$, $P < 0.01$; Tukey HSD *post hoc* comparison, $P < 0.05$ Fig. 2; $n = \geq 20$ cells per group), showing that day–night differences in this current is specific to increased levels of GIRK2 (Fig. 2).

GIRK channels are known to decrease cellular excitability by hyperpolarizing the membrane (Luscher & Slesinger, 2010). To determine whether loss of GIRK2 plays a role in regulating SCN neuronal membrane properties, we measured resting membrane potential (RMP) of WT and KO SCN neurons during the day and night ($n = \geq 25$ cells per group). Consistent with previous results (Kuhlman & McMahon, 2004), there was an overall day–night difference in RMP (Kruskal–Wallis test, $H_{(3)} = 37.403$, $P < 0.01$; median *post hoc* test, $P < 0.05$ for both WT day compared to night, and KO day compared to night; Fig. 3*A* and *B*). As predicted, KO neurons were significantly more depolarized than WT neurons during the day only (WT day: -41.6 ± 1.0 mV; KO day: -36.5 ± 1.1 mV; median *post hoc* test, $P < 0.05$). To eliminate the possibility that the depolarized RMP in KO mice was driven by altered regulation of ion channel expression to compensate for loss of GIRK2, we applied a GIRK channel antagonist, Tertiapin-Q (TPQ, $0.2\ \mu$M), to WT slices during the day (Fig. 3*B*). We found that TPQ caused a similar magnitude of depolarization (-36.9 ± 1.0 mV, $n = 38$ cells), demonstrating that GIRK channels are necessary for maintaining normal day-time resting membrane potential. There were no significant differences in either input resistance (Kruskal–Wallis test, $H_{(3)} = 2.662$, $P > 0.05$), action potential firing rate (Kruskal Wallis test, $H_{(3)} = 4.879$, $P > 0.05$), or peak current amplitude of action potential firing (Kruskal–Wallis test, $H_{(3)} = 2.744$, $P > 0.05$) among groups (Fig. 3*C–E*), indicating that GIRK channels primarily regulate resting membrane potential.
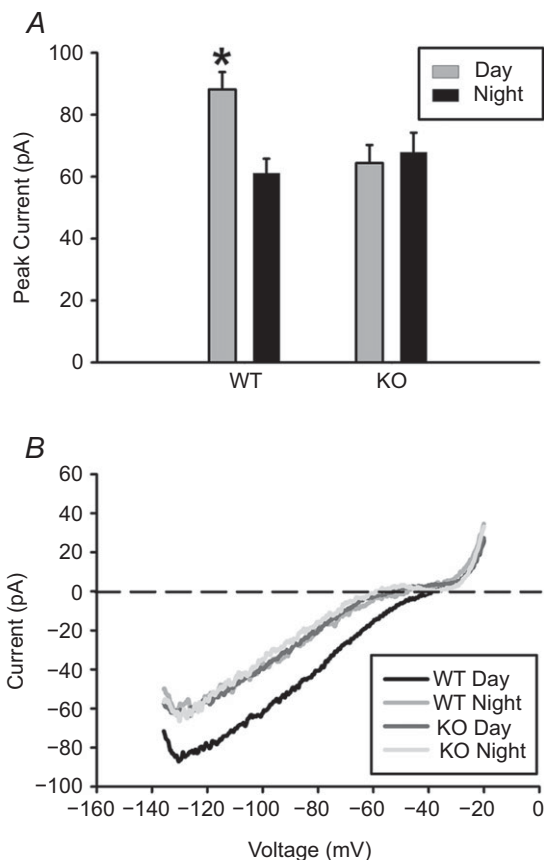
Loss of GIRK2 alters the behavioural response to non-photic and photic cues

After defining the temporal pattern of GIRK subunit expression and describing a role for GIRK channels in setting day-time resting membrane potential, we next evaluated the functional role of GIRK2 in the entrainment of behavioural locomotor rhythms. There were no behavioural differences between heterozygous and WT animals (data not shown), and therefore, the following results are from WT–KO comparisons only. First, we examined general cage activity of mice single-housed with the running wheel locked because several studies have shown that wheel running (a non-photic entraining stimulus) shortens the period of behavioural locomotor rhythms in DD (Edgar *et al.* 1991*a*,*b*; Kuroda *et al.* 1997; Deboer & Tobler, 2000; Harrington *et al.* 2007). Activity monitored with infrared motion sensors revealed no significant differences between genotypes in terms of average activity counts or circadian rhythmic amplitude in LD (Fig. 4*A* and *B*; Table 1). In addition, WT and KO mice had very similar period lengths (or tau) when placed into DD (Table 1, $n = 15$–16 per group). To test whether loss of GIRK2 alters the period shortening response to the non-photic stimulus of wheel running (Harrington *et al.* 2007), we placed WT and KO animals on running wheels and assessed tau in DD (Fig. 4*B* and *C*). In an LD cycle, there was no difference between KO and WT average activity counts (Table 1). In DD, KO animals had higher daily activity in general (Table 1); however, this effect was

Figure 2. GIRK currents are increased during the day in SCN neurons
A, peak inward current (mean ± SEM) during the day *vs.* night (**P* < 0.05) for GIRK2 knockout (KO) and wild-type (WT) mice. *B*, representative voltage-clamp ramp traces. Recordings were done in the presence of TTX (1 μM), bicuculline (30 μM), D-AP5 (50 μM), CNQX (10 μM), and CdCl$_2$ (200 μM) in order to block synaptic transmission. All recordings were done in 30 mM KCl to increase potassium conductance. *n* = at least 3 animals and 20 cells per group.

mostly driven by increased activity of KO mice during the subjective night (mean ± SEM counts, WT night: 2867.5 ± 303.0, KO night: 3996.6 ± 252.7) but not during the day (mean ± SEM counts, WT day: 287.2 ± 37.9, KO day: 296.0 ± 60.5) consistent with reports of hyperactivity in these mice (Blednov *et al.* 2001). A repeated measures ANOVA revealed a significant

time-of-day by genotype interaction ($F_{(2,21)} = 4.906$, $P < 0.05$) with KO night activity significantly greater than WT night activity (Tukey HSD *post hoc* comparison, $P < 0.05$; Fig. 4*B* and *C*). In contrast to general cage activity, KO mice with access to a running wheel did not exhibit the shorter free running period observed in WT mice (mean ± SEM, WT: 23.80 ± 0.04 h, KO: 23.95 ± 0.04 h;
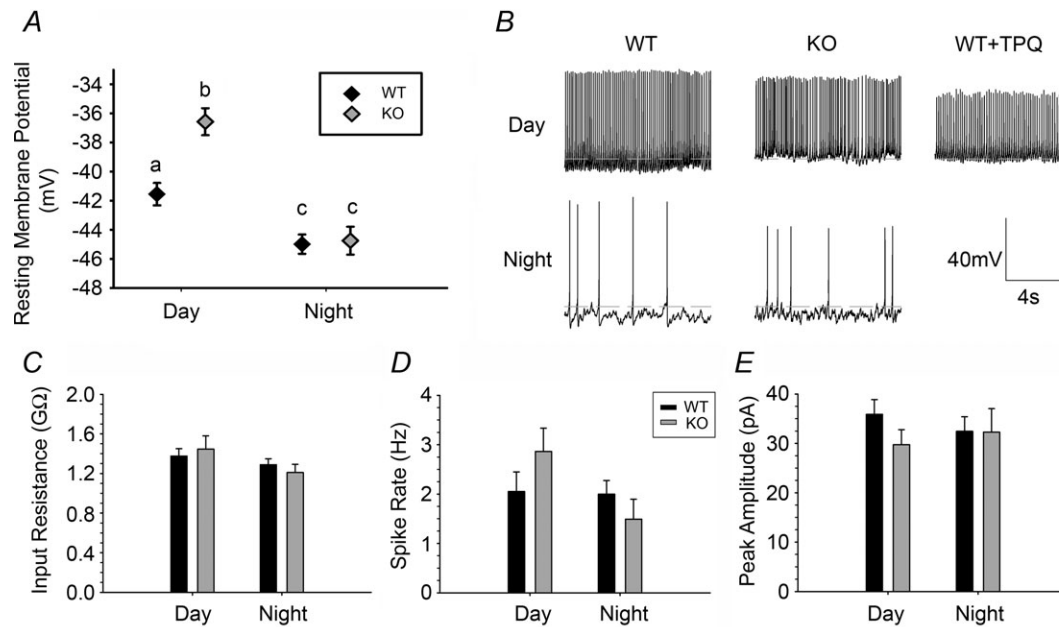

Figure 3. GIRK2 knockout SCN neurons exhibit more depolarized resting membrane potential compared to wild-type controls
A, resting membrane potential of WT and KO SCN neurons during the day and night. Lowercase letters (a, b, c) indicate groups that are significantly different (*$P < 0.05$). *B*, representative gap-free current clamp of KO and WT SCN neurons during the day and at night. A representative trace from WT slices treated with the GIRK2 antagonist Tertiapin-Q (0.2 μM) during the day is also included. Dotted line indicates −40 mV. *C–E*, input resistance, action potential frequency from gap-free current clamp recordings, and action potential amplitudes from gap-free current clamp recordings, respectively, from WT and KO neurons during the day and night. $n = 3–5$ animals and at least 25 cells per group.
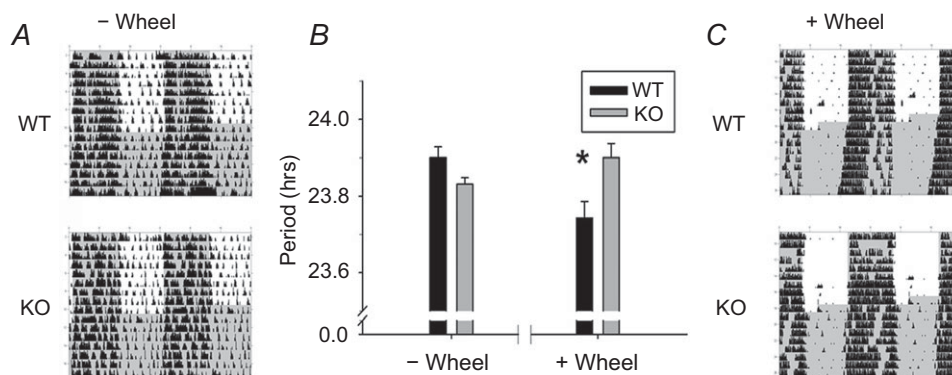

**Figure 4. GIRK2 knockout mice fail to shorten free-running period in response to wheel-running activity**
A, representative, double-plotted actograms of WT (top) and KO (bottom) mice without wheel access (activity measured by infrared motion sensors), $n = 14–15$ per group. *B*, wheel-locked infrared free-running period (mean ± SEM), and wheel-running activity-based free-running period (mean ± SEM) for KO and WT mice. *$P < 0.05$. *C*, representative actograms for WT and KO mice with wheel access (right, activity measured by wheel revolutions); $n = 7–8$ animals per each group. Time of lights off is indicated by dark grey; black tick marks indicate activity counts.

Table 1. Circadian behavioural analysis of GIRK2 KO mice

			WT		KO		Independent samples t test		
			Mean	SEM	Mean	SEM	t	d.f.	Significance (2-tailed)
No wheel	LD	Power	705.21	54.07	646.28	42.49	−0.86	24	0.400
		Mean counts (counts min^{-1})	3.02	0.26	2.56	0.18	−1.44	24	0.164
	DD	Tau	23.92	0.04	23.85	0.04	−1.08	24	0.292
		Power	539.24	2.79	534.05	28.64	−0.15	24	0.885
		Mean counts (counts min^{-1}	2.91	0.20	2.87	0.20	−0.11	24	0.913
Wheel	LD	Power	1099.6	59.83	1170.3	118.43	0.55	13	0.589
		Mean counts (counts min^{-1})	14.51	1.98	16.13	1.87	0.59	13	0.566
	DD	Tau	23.80	0.04	23.95	0.04	2.46	13	0.029
		Power	1174	86.84	1430.7	86.55	2.08	13	0.058
		Mean counts (counts min^{-1})	11.85	1.65	18.72	1.95	0.76	13	0.018

$t_{(13)} = 2.46$, $P < 0.05$, $n = 7$–8 per group; $\eta^2 = 0.32$) indicating that GIRK2 is necessary for proper non-photic signalling in response to wheel running.

Because the behavioural response to non-photic cues was altered upon loss of GIRK2, we examined whether GIRK2 contributes to photic entrainment as well. Mice housed in a 12 h:12 h LD cycle were subjected to a 6 h phase advance of the LD cycle (Fig. 5), and the number of days required for re-entrainment was determined.

A

B   WT   KO
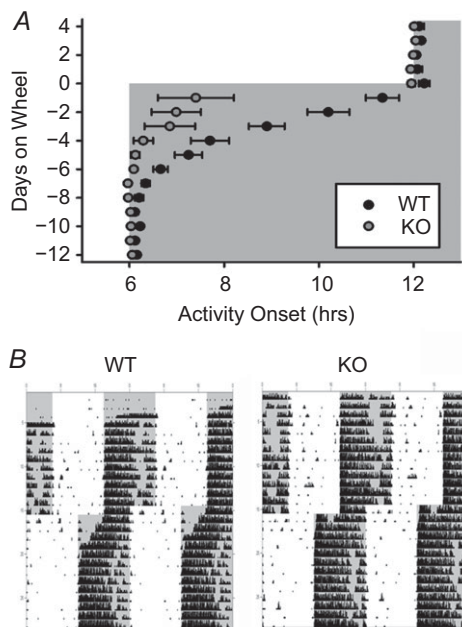
Figure 5. GIRK2 knockout mice entrain more rapidly to a 6 h light cycle advance
A, activity onset (mean ± SEM) in days prior and following a 6 h advance of an LD cycle (day 0) for WT and KO mice. Lights off represented by grey shading. *B*, representative actograms of WT (left) and KO (right) mice housed on wheels in a 12 h:12 h LD cycle. Lights off represented by grey shading; black tick marks indicate activity counts. $n = 6$ animals per group.

Entrainment was defined as the first day in which the activity length returned to the same length observed before the light shift (see Methods). Mice lacking GIRK2 required approximately half the number of days to re-entrain to the new light cycle compared to WT (mean ± SEM days to entrain, WT: 7.2 ± 0.5, KO: 3.5 ± 0.8; $t_{(10)} = 4.07$, $P < 0.01$; $n = 6$ per group). However, KO mice entrained to a 6 h phase delay at the same rate as WT (mean ± SEM days to entrain, WT: 4.7 ± 0.7, KO: 4.7 ± 0.5; $t_{(10)} = -0.23$, $P > 0.05$; $n = 6$ per group). These results indicate that GIRK2 signalling slows the rate of re-entrainment to photic phase advances, but not delays.

Neuropeptide Y signalling in the SCN requires GIRK2

In rodents, disruption of the non-photic neurotransmitter NPY abolishes the period shortening effect of wheel access (Pickard *et al.* 1987; Pickard, 1994; Kuroda *et al.* 1997; Lewandowski & Usarek, 2002; Harrington *et al.* 2007). Because NPY signalling also antagonizes phase advances to light (Yannielli & Harrington, 2000; Lall & Biello, 2003; Yannielli *et al.* 2004), disruption of the NPY-dependent non-photic signalling pathway may explain the loss of wheel running-induced period shortening and the enhanced photic entrainment of KO mice. Specifically, we hypothesized that NPY-induced phase shifts within the SCN requires GIRK2 activation because application of NPY to the SCN *in vivo* or *in vitro* during the day induces phase advances in behaviour and neuronal activity rhythms (Yannielli & Harrington, 2000; Maywood *et al.* 2002; Lall & Biello, 2003; Yannielli *et al.* 2004; Besing *et al.* 2012) and NPY-induced effects in other brain regions require GIRK activation (Paredes *et al.* 2003; Fu *et al.* 2004).

First, we investigated whether the suppressive effects of NPY on SCN neuron firing rate (van den Pol *et al.* 1996;

Besing *et al.* 2012) were lost in GIRK2 KO mice using loose patch electrophysiology with and without 2.35 μM NPY in the bath ($n = \geq 45$ cells per group). Spontaneous firing rate was significantly different among the four groups (Kruskal–Wallis test, $H_{(3)} = 79.271$, $P < 0.01$). Surprisingly, firing rates of WT and KO neurons did not differ (median *post hoc* test, $P > 0.05$; Fig. 6A); however, KO neurons exhibited significantly higher firing rates than WT neurons in response to NPY (mean $\pm$ SEM, WT: 0.8 ± 0.2 Hz, KO: 2.2 ± 0.3 Hz; median *post hoc* test, $P < 0.01$; Fig. 6A and B). Contingency analysis revealed a significant effect of genotype and treatment on the percentage of silent cells ($\chi^2_{(3)} = 53.193$, $P < 0.01$). Specifically, in vehicle-treated slices, the number of silent cells was not significantly different between KO and WT (Fisher's exact test, $P > 0.05$); however, WT slices treated with NPY had significantly more silent cells than did NPY-treated KO slices (Fisher's exact test, $P < 0.01$; Fig. 6B and C), suggesting that NPY failed to silence many of the SCN neurons in the absence of GIRK2. In order to determine whether GIRK channels directly mediate NPY-induced current, gap-free, whole-cell voltage clamp was used to hold the cells at -80 mV in high potassium (30 mM) in order to readily measure the GIRK-mediated current (as in (Hamasaki *et al.* 2013)). Upon application of NPY (2.35 μM), 4 out of 5 cells responded to NPY with inward current (range, 15–119 pA; mean $\pm$ SEM, 44.5 ± 23.2 pA, $n = 4$ cells from two animals). Of these, three out of four cells had reduced inward current by ∼50% in response to TPQ (0.2 μM). TPQ alone had a net inward current of 3.1 ± 4.4 pA ($n = 4$ cells from two animals). These results indicate that GIRK channels mediate at least part of the NPY-induced current within SCN neurons, consistent with the partial effect of NPY in the GIRK2 KO animals (Fig. 6). This failure to significantly reduce excitability in GIRK2 KO animals may impede NPY-dependent phase shifts to the circadian clock.

To test this hypothesis, we crossed GIRK2 WT and KO animals onto the *Per2^{Luc+/-}* reporter line (see Methods) and measured the phase shifting effect of NPY on the molecular clock. Because these animals showed no difference in behavioural circadian rhythmicity (Fig. 4), it was not surprising that the PER2::LUC rhythms showed no difference in period between genotypes pre-treatment (mean period $\pm$ SEM, WT: 24.42 ± 0.12 h, KO: 24.38 ± 0.16 h; $t_{(28)} = 0.99$, $P > 0.05$). As has been previously reported by Besing *et al.* (2012) and more recently by Belle *et al.* (2014), 1 h treatment with 2.35 μM NPY during the early day (CT 4–5) produced ∼3 h phase advances in PER2::LUC rhythms in WT mice; however, phase advances in KO animals were reduced to the level of controls (two-way ANOVA, genotype by treatment interaction: $F_{(1,26)} = 4.77$, $P < 0.05$; Tukey HSD *post hoc*, $P < 0.05$, Fig. 7; $n = 6$–8 cultures per group). Thus, these results suggest that GIRK2 is necessary for NPY-induced phase advances within the SCN, and that loss of NPY signalling may be an underlying cause for the circadian entrainment alterations observed in GIRK2 KO mice.

GIRK channel activation is sufficient to cause a non-photic-like phase shift

We have shown that GIRK channels partially mediate NPY-induced silencing of SCN neurons as well as NPY-induced phase advances of the molecular clock. However, GIRK channels can be fully opened by a variety of neurotransmitter signalling (Luscher & Slesinger, 2010), including other non-photic signals. To test the hypothesis that GIRK channel activation was sufficient to mimic non-photic signals, we applied 10 μM ML297, a GIRK channel agonist (Days *et al.* 2010; Kaufmann *et al.* 2013), for 1 h to PER2::LUC SCN cultures starting between CT 3 and CT 4. This concentration was sufficient to induce GIRK currents in SCN neurons (-60.3 ± 9.7 pA, $n = 3$ cells), consistent with recent papers demonstrating ML297 specificity in cultured hippocampal neurons (Wydeven *et al.* 2014). Activation of GIRK channels with ML297 significantly phase advanced PER2::LUC rhythms compared to vehicle-treated controls (mean $\pm$ SEM, ML297: 3.6 ± 1.1 h, vehicle: 0.3 ± 0.2 h; $t_{(5.23)} = -3.10$,
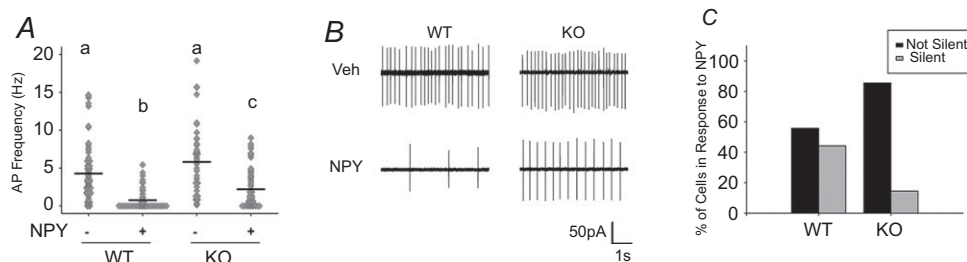

Figure 6. Loss of GIRK2 reduces effect of NPY on SCN neuron spontaneous firing rate
A, frequency plot of individual WT and KO SCN neurons treated with 2.35 μM NPY or vehicle from ZT 4 to 6. Mean value indicated by black continuous line. Lowercase letters (a, b, c) indicate groups that are significantly different (*$P < 0.05$). *B*, representative loose patch traces (5 s) of neurons in *A*. *C*, percentage of silent cells *vs.* non-silent cells with NPY treatment. $n = 3$ animals and ≥ 45 cells per group.

$P < 0.05$; Fig. 8; $n = 6$ cultures per group), suggesting a broader role for GIRK channels in mediating non-photic signals.

Discussion

Although G protein signalling is critical for circadian rhythmicity (Cheng *et al.* 2004; Aton *et al.* 2006; Zuberi *et al.* 2008; Doi *et al.* 2011; Brancaccio *et al.* 2013), the role of G protein-coupled potassium channels, and specifically GIRK channels, in modulating time-of-day cues has not been studied. This paper is the first to show that a single, circadian-regulated GIRK channel subunit can modulate SCN neurophysiology, mediate the effects of day-time NPY, and alter behaviour in response to both photic and non-photic cues. Specifically, we found that GIRK2 protein and function exhibited an endogenous rhythm within the SCN with a peak around midday. This increase during the day was necessary for proper maintenance of day-time resting membrane potential within SCN neurons since GIRK channel inhibition or GIRK2 knockout further depolarized resting membrane potential. Furthermore, animals with genetic loss of GIRK2 showed altered entrainment properties, such that the GIRK2 KO animals (compared to WT mice) re-entrained to a 6 h phase advance of the light–dark cycle more rapidly and did not exhibit period shortening with wheel access. These behavioural phenotypes may be due, in part, to a loss of NPY signalling within the SCN as indicated by the reduced effects of NPY on firing rate of SCN neurons in GIRK2 KO animals as well as impaired NPY-induced phase advances in GIRK2 KO organotypic cultures of the SCN. Finally, GIRK channel activation was sufficient to cause a day-time phase advance in PER2::LUC rhythms. Taken together, the results of our study indicate a role for circadian regulation of GIRK

channels in modulation of neurophysiological rhythms and establishing proper responses to time-of-day stimuli.

The circadian regulation of neural activity in SCN neurons has been well documented with peak excitation occurring during the day (Kuhlman & McMahon, 2006). GIRK channels are inwardly rectifying and can be identified as an inward potassium current at greatly hyperpolarized potentials (beyond physiological resting membrane potential). At more depolarized potentials in the physiological range of most neurons, GIRK channels pass an outward potassium current, causing membrane hyperpolarization and decreased neuronal excitability (Luscher & Slesinger, 2010). In the present study, GIRK2 channel protein and current was highest during the day (Figs 1 and 2). Therefore, we hypothesized that GIRK channel activation during the day may act as a stop-gate on excitability. Indeed, we found that loss of GIRK2 channels or pharmacological GIRK channel inhibition resulted in depolarization of the resting membrane potential by ~5 mV (Fig. 3). This basal GIRK-mediated hyper-polarization is consistent with the effects of GIRK channel activation by neurotransmitters such as NPY, serotonin, melatonin, glutamate, acetylcholine, and GABA in a variety of central and peripheral areas (Krapivinsky *et al.* 1995; Nelson *et al.* 1996; Luscher *et al.* 1997; Fu *et al.* 2004; Acuna-Goycolea *et al.* 2005; Luscher & Slesinger, 2010). For example, GIRK channels have been shown to couple directly with $GABA_B$ receptors (Luscher *et al.* 1997; Arora *et al.* 2011), and GABA signalling within the SCN is dependent upon $G_{i/o}$ G proteins (Aton *et al.* 2006) which are necessary for GIRK channel opening.

The neurotransmitters listed above also play key roles in regulating the timing of circadian rhythms (Albrecht, 2012). Underlying mechanisms of non-photic entrainment, or synchronization of rhythms to cues like
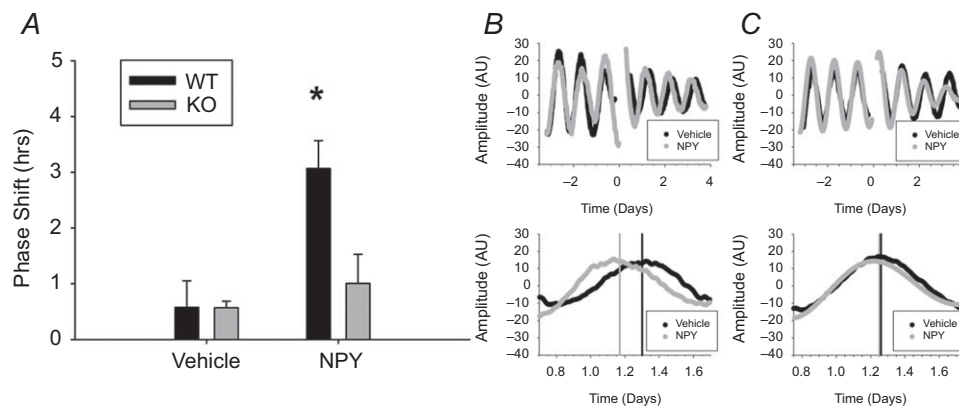

Figure 7. GIRK2 is necessary for NPY-induced phase shifts in the molecular clock
A, phase shifts of PER2::LUC rhythms in response to a 1 h treatment of 2.35 μM NPY or vehicle at CT 4 in WT and KO mice. *$P < 0.05$. *B* and *C*, representative bioluminescence traces from two WT (*B*) or two KO (*C*) SCN cultures treated with vehicle (black) or NPY (grey) for three cycles before and after treatment (top) or day 1 after treatment (bottom). Time 0: onset of NPY application. Predicted peak time, determined from 3 cycles post treatment, is indicated by vertical bars for each group. $n = 6$–8 cultures per group.

exercise or stress, remain largely understudied even though they block the effects of light and reset clock phase both in rodents and humans (Hastings *et al.* 1998; Mistlberger & Skene, 2005). For example, both melatonin and NPY induce large phase advances of locomotor behaviour and spike rate rhythms during the day and hyperpolarize the resting membrane potential in a potassium-sensitive manner (Jiang *et al.* 1995; Hall *et al.* 1999; Scott *et al.* 2010). Our results showed that GIRK2 activation was necessary and sufficient to induce these large non-photic-like phase advances of the molecular clock (Figs 6 and 8). It is interesting to note that both NPY and melatonin hyperpolarize the membrane and reduce spontaneous firing rate of SCN neurons when treated during the subjective day (Jiang *et al.* 1995; Hall *et al.* 1999; Scott *et al.* 2010). Based on these observations, it can be speculated that these channels mediate multiple phase-resetting signals and may act as a convergence point for non-photic signalling, resulting in similar phase response curves for serotonin, NPY, and melatonin (Yannielli & Harrington, 2004). An important function of increased GIRK current during the day could be to allow for daytime environmental cues to phase shift

Figure 8. Activation of GIRK channels induces non-photic-like phase advances
A, phase shifts of PER2::LUC rhythms in response to a 1 h treatment of 10 μM ML297 or vehicle starting between CT 3–4.5. *B*, representative bioluminescence traces from SCN cultures treated with vehicle (black) or ML297 (grey) for three cycles before and after treatment. *n* = 6 cultures per group.

the SCN through hyperpolarization. This hypothesis is supported by the fact that activation of GIRK channels with ML297 during the early day is sufficient to cause a phase advance of molecular clock rhythms (Fig. 8). However, GIRK channel activation does not preclude possible co-activation of second messenger signalling cascades by non-photic cues such as PKC activation in response to NPY (Biello *et al.* 1997). Indeed, NPY still has a partial effect on spike rate in GIRK2 KO animals (Fig. 6).

Photic and non-photic entraining stimuli can interact and in general are mutually inhibitory. For example, NPY injection into the SCN region of light-exposed hamsters in the late night attenuates the characteristically ensuing phase advance and up-regulation of clock gene expression (Yannielli *et al.* 2004; Gamble *et al.* 2006). Conversely, NPY blockade of NPY Y5 receptors enhance light-induced phase advances (Yannielli *et al.* 2004). Similar experiments have been done with light mimicked by the glutamate receptor agonist NMDA, such that phase advances in SCN firing or wheel running behaviour were diminished by NPY and NPY receptor agonists (Gamble *et al.* 2004; Soscia & Harrington, 2004, 2005; Yannielli & Harrington, 2004). In addition to acute phase shifts, NPY is also critical for other non-photic behavioural effects, such as period shortening in response to wheel running. Elimination of the primary source of NPY to the SCN through lesions of the intergeniculate leaflet blocks period shortening induced by wheel access (Pickard *et al.* 1987; Pickard, 1994; Kuroda *et al.* 1997; Lewandowski & Usarek, 2002). This result is consistent with more recent evidence that NPY-deficient mice also fail to shorten free running period in response to wheel access (Harrington *et al.* 2007). The present data suggest that GIRK channel activation may be involved in these phenotypes. Specifically, loss of GIRK2 channels resulted in a lack of period shortening typically observed in response to non-photic wheel access (Fig. 5) as well as enhanced phase advances in the light–dark cycle (Fig. 4). It appears that in the absence of GIRK signalling, entrainment to photic phase advances are functionally enhanced, while the non-photic pathway is suppressed. Because there was no change in entrainment to photic delays, future studies should determine whether this photic phenotype is a broad strengthening of photic entrainment pathway, or simply a removal of non-photic inhibition to photic phase advances in behaviour. In addition, future studies should examine the role of GIRK in retinal ganglion cells and within intergeniculate leaflet given its wide-spread expression in neurons (Signorini *et al.* 1997; Luscher & Slesinger, 2010). A better understanding of the non-photic–photic interaction is an important area for future research given that an animal is unlikely to encounter a photic or non-photic stimulus in isolation.
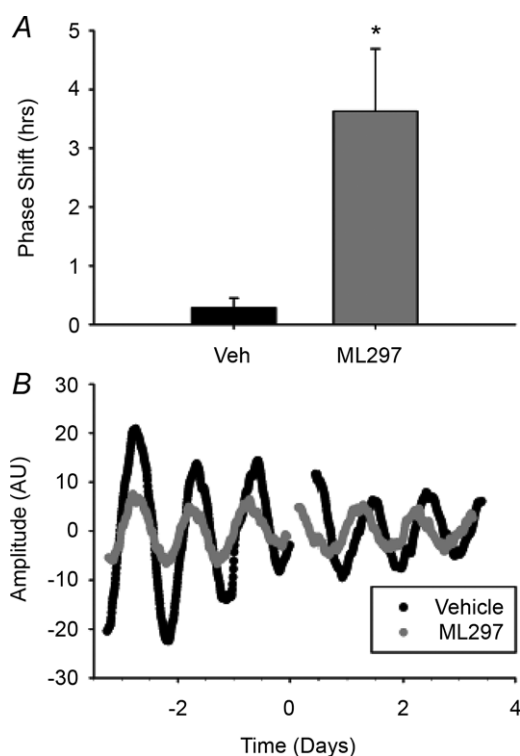
In the present study, we found that both GIRK2 protein expression and current amplitude were regulated over the day–night cycle. This result is consistent with the finding that GIRK2 mRNA expression in microarrays of SCN tissue is rhythmic (Pizarro *et al.* 2013), indicating that the gene transcribing GIRK2 mRNA (KCNJ6) may be under direct clock control. In general, our understanding of the mechanisms underlying circadian regulation of ion channels is limited (Colwell, 2011), but some studies suggest epigenetic mechanisms or microRNA modifications may determine transcript stability (Wang, 2013), while other studies have shown that free radical homeostasis can also regulate ion channel gating (Wang *et al.* 2012). Determining clock control of ionic channel regulation in the SCN could provide insight into how ion channels are regulated in a circadian manner in other brain areas and tissues. GIRK channels have been implicated in regulating dopamine signalling within the ventral tegmental area (Lomazzi *et al.* 2008; Arora *et al.* 2011). If GIRK channels are regulated in a time-of-day-sensitive manner in the ventral tegmental area (as in the SCN) then the present results may have broader implications for addiction and withdrawal and the circadian regulation of this disease.

GIRK channels have also been associated in diseases of hyper-excitability such as epilepsy (Loddenkemper *et al.* 2011; Zarowski *et al.* 2011), chronic atrial fibrillation (Capucci *et al.* 2012; Shusterman *et al.* 2012), and long QT syndrome (Jeyaraj *et al.* 2012; Takigawa *et al.* 2012). A key feature these disorders is that seizure or fibrillation onset is more likely to occur during the day in humans, suggesting that circadian control of GIRK channel function may underlie risk dependence on time of day. Indeed, microarray studies have shown that GIRK1 and GIRK4 transcripts are rhythmic in mouse whole-heart homogenate (Pizarro *et al.* 2013). Perhaps by understanding the interplay between GIRK channel dysfunction and circadian regulation of excitability throughout the body, novel time-of-day-sensitive therapeutics could be developed with fewer off-target effects.

References

Acuna-Goycolea C, Tamamaki N, Yanagawa Y, Obata K & van den Pol AN (2005). Mechanisms of neuropeptide Y, peptide YY, and pancreatic polypeptide inhibition of identified green fluorescent protein-expressing GABA neurons in the hypothalamic neuroendocrine arcuate nucleus. *J Neurosci* **25**, 7406–7419.

Aguado C, Colon J, Ciruela F, Schlaudraff F, Cabanero MJ, Perry C, Watanabe M, Liss B, Wickman K & Lujan R (2008). Cell type-specific subunit composition of G protein-gated potassium channels in. *J Neurochem* **105**, 497–511.

Albrecht U (2012). Timing to perfection: the biology of central and peripheral circadian clocks. *Neuron* **74**, 246–260.

Arora D, Hearing M, Haluk DM, Mirkovic K, Fajardo-Serrano A, Wessendorf MW, Watanabe M, Lujan R & Wickman K (2011). Acute cocaine exposure weakens GABA$_B$ receptor-dependent G-protein-gated inwardly rectifying K$^+$ signaling in dopamine neurons of the ventral tegmental area. *J Neurosci* **31**, 12251–12257.

Aton SJ, Huettner JE, Straume M & Herzog ED (2006). GABA and Gi/o differentially control circadian rhythms and synchrony in clock neurons. *Proc Natl Acad Sci U S A* **103**, 19188–19193.

Belle MD, Hughes AT, Bechtold DA, Cunningham P, Pierucci M, Burdakov D & Piggins HD (2014). Acute suppressive and long-term phase modulation actions of orexin on the mammalian circadian clock. *J Neurosci* **34**, 3607–3621.

Besing RC, Hablitz LM, Paul JR, Johnson RL, Prosser RA & Gamble KL (2012). Neuropeptide Y-induced phase shifts of PER2::LUC rhythms are mediated by long-term suppression of neuronal excitability in a phase-specific manner. *Chronobiol Int* **29**, 91–102.

Biello SM (2009). Circadian clock resetting in the mouse changes with age. *Age (Dordr)* **31**, 293–303.

Biello SM, Golombek DA, Schak KM & Harrington ME (1997). Circadian phase shifts to neuropeptide Y *in vitro*: cellular communication and signal transduction. *J Neurosci* **17**, 8468–8475.

Blednov YA, Stoffel M, Chang SR & Harris RA (2001). GIRK2 deficient mice. Evidence for hyperactivity and reduced anxiety. *Physiol Behav* **74**, 109–117.

Brancaccio M, Maywood ES, Chesham JE, Loudon AS & Hastings MH (2013). A Gq–Ca^{2+} axis controls circuit-level encoding of circadian time in the suprachiasmatic nucleus. *Neuron* **78**, 714–728.

Bray MS, Ratcliffe WF, Grenett MH, Brewer RA, Gamble KL & Young ME (2013). Quantitative analysis of light-phase restricted feeding reveals metabolic dyssynchrony in mice. *Int J Obes (Lond)* **37**, 843–852.

Capucci A, Calcagnini G, Mattei E, Triventi M, Bartolini P, Biancalana G, Gargaro A, Puglisi A & Censi F (2012). Daily distribution of atrial arrhythmic episodes in sick sinus syndrome patients: implications for atrial arrhythmia monitoring. *Europace* **14**, 1117–1124.

Cheng HY, Obrietan K, Cain SW, Lee BY, Agostino PV, Joza NA, Harrington ME, Ralph MR & Penninger JM (2004). Dexras1 potentiates photic and suppresses nonphotic responses of the circadian clock. *Neuron* **43**, 715–728.

Colwell CS (2011). Linking neural activity and molecular oscillations in the SCN. *Nat Rev Neurosci* **12**, 553–569.

Dahdal D, Reeves DC, Ruben M, Akabas MH & Blau J (2010). Drosophila pacemaker neurons require G-protein signaling and GABAergic inputs to generate 24hr behavioral rhythms. *Neuron* **68**, 964–977.

Days E, Kaufmann K, Romaine I, Niswender C, Lewis M, Utley T, Du Y, Sliwoski G, Morrison R, Dawson ES, Engers JL, Denton J, Daniels JS, Sulikowski GA, Lindsley CW & Weaver CD (2010). Discovery and characterization of a selective activator of the g-protein activated inward-rectifying potassium (GIRK) channel. In *Probe Reports from the NIH Molecular Libraries Program*. National Center for Biotechnology Information (US), Bethesda, MD, USA.

Deboer T & Tobler I (2000). Running wheel size influences circadian rhythm period and its phase shift in mice. *J Comp Physiol A* **186**, 969–973.

Doi M, Ishida A, Miyake A, Sato M, Komatsu R, Yamazaki F, Kimura I, Tsuchiya S, Kori H, Seo K, Yamaguchi Y, Matsuo M, Fustin JM, Tanaka R, Santo Y, Yamada H, Takahashi Y, Araki M, Nakao K, Aizawa S, Kobayashi M, Obrietan K, Tsujimoto G & Okamura H (2011). Circadian regulation of intracellular G-protein signalling mediates intercellular synchrony and rhythmicity in the suprachiasmatic nucleus. *Nat Commun* **2**, 327.

Edgar DM, Kilduff TS, Martin CE & Dement WC (1991*a*). Influence of running wheel activity on free-running sleep/wake and drinking circadian rhythms in mice. *Physiol Behav* **50**, 373–378.

Edgar DM, Martin CE & Dement WC (1991*b*). Activity feedback to the mammalian circadian pacemaker: influence on observed measures of rhythm period length. *J Biol Rhythms* **6**, 185–199.

Fu LY, Acuna-Goycolea C & van den Pol AN (2004). Neuropeptide Y inhibits hypocretin/orexin neurons by multiple presynaptic and postsynaptic mechanisms: tonic depression of the hypothalamic arousal system. *J Neurosci* **24**, 8741–8751.

Gamble KL, Novak CM & Albers HE (2004). Neuropeptide Y and *N*-methyl-D-aspartic acid interact within the suprachiasmatic nuclei to alter circadian phase. *Neuroscience* **126**, 559–565.

Gamble KL, Paul KN, Karom MC, Tosini G & Albers HE (2006). Paradoxical effects of NPY in the suprachiasmatic nucleus. *Eur J Neurosci* **23**, 2488–2494.

Hall AC, Earle-Cruikshanks G & Harrington ME (1999). Role of membrane conductances and protein synthesis in subjective day phase advances of the hamster circadian clock by neuropeptide Y. *Eur J Neurosci* **11**, 3424–3432.

Hamasaki R, Shirasaki T, Soeda F & Takahama K (2013). Tipepidine activates VTA dopamine neuron via inhibiting dopamine D_2 receptor-mediated inward rectifying K^+ current. *Neuroscience* **252**, 24–34.

Harrington M, Molyneux P, Soscia S, Prabakar C, McKinley-Brewer J & Lall G (2007). Behavioral and neurochemical sources of variability of circadian period and phase: studies of circadian rhythms of *npy*–/– mice. *Am J Physiol Regul Integr Comp Physiol* **292**, R1306–R1314.

Hastings MH, Duffield GE, Smith EJ, Maywood ES & Ebling FJ (1998). Entrainment of the circadian system of mammals by nonphotic cues. *Chronobiol Int* **15**, 425–445.

Hibino H, Inanobe A, Furutani K, Murakami S, Findlay I & Kurachi Y (2010). Inwardly rectifying potassium channels: their structure, function, and physiological roles. *Physiol Rev* **90**, 291–366.

Jeyaraj D, Haldar SM, Wan X, McCauley MD, Ripperger JA, Hu K, Lu Y, Eapen BL, Sharma N, Ficker E, Cutler MJ, Gulick J, Sanbe A, Robbins J, Demolombe S, Kondratov RV, Shea SA, Albrecht U, Wehrens XH, Rosenbaum DS & Jain MK (2012). Circadian rhythms govern cardiac repolarization and arrhythmogenesis. *Nature* **483**, 96–99.

Jiang ZG, Nelson CS & Allen CN (1995). Melatonin activates an outward current and inhibits I_h in rat suprachiasmatic nucleus neurons. *Brain Res* **687**, 125–132.

Kaufmann K, Romaine I, Days E, Pascual C, Malik A, Yang L, Zou B, Du Y, Sliwoski G, Morrison RD, Denton J, Niswender CM, Daniels JS, Sulikowski GA, Xie XS, Lindsley CW & Weaver CD (2013). ML297 (VU0456810), the First potent and selective activator of the GIRK potassium channel, displays antiepileptic properties in mice. *ACS Chem Neurosci* **4**, 1278–1286.

Koyrakh L, Lujan R, Colon J, Karschin C, Kurachi Y, Karschin A & Wickman K (2005). Molecular and cellular diversity of neuronal G-protein-gated potassium channels. *J Neurosci* **25**, 11468–11478.

Krapivinsky G, Gordon EA, Wickman K, Velimirovic B, Krapivinsky L & Clapham DE (1995). The G-protein-gated atrial K^+ channel I_{KACh} is a heteromultimer of two inwardly rectifying K^+-channel proteins. *Nature* **374**, 135–141.

Kuhlman SJ & McMahon DG (2004). Rhythmic regulation of membrane potential and potassium current persists in SCN neurons in the absence of environmental input. *Eur J Neurosci* **20**, 1113–1117.

Kuhlman SJ & McMahon DG (2006). Encoding the ins and outs of circadian pacemaking. *J Biol Rhythms* **21**, 470–481.

Kuhlman SJ, Silver R, Le Sauter J, Bult-Ito A & McMahon DG (2003). Phase resetting light pulses induce Per1 and persistent spike activity in a subpopulation of biological clock neurons. *J Neurosci* **23**, 1441–1450.

Kuroda H, Fukushima M, Nakai M, Katayama T & Murakami N (1997). Daily wheel running activity modifies the period of free-running rhythm in rats via intergeniculate leaflet. *Physiol Behav* **61**, 633–637.

Lall GS & Biello SM (2003). Attenuation of circadian light induced phase advances and delays by neuropeptide Y and a neuropeptide Y Y1/Y5 receptor agonist. *Neuroscience* **119**, 611–618.

Lesage F, Guillemare E, Fink M, Duprat F, Heurteaux C, Fosset M, Romey G, Barhanin J & Lazdunski M (1995). Molecular properties of neuronal G-protein-activated inwardly rectifying K^+ channels. *J Biol Chem* **270**, 28660–28667.

Lewandowski MH & Usarek A (2002). Effects of intergeniculate leaflet lesions on circadian rhythms in the mouse. *Behav Brain Res* **128**, 13–17.

Loddenkemper T, Vendrame M, Zarowski M, Gregas M, Alexopoulos AV, Wyllie E & Kothare SV (2011). Circadian patterns of pediatric seizures. *Neurology* **76**, 145–153.

Lomazzi M, Slesinger PA & Luscher C (2008). Addictive drugs modulate GIRK-channel signaling by regulating RGS proteins. *Trends Pharmacol Sci* **29**, 544–549.

Luscher C, Jan LY, Stoffel M, Malenka RC & Nicoll RA (1997). G protein-coupled inwardly rectifying K^+ channels (GIRKs) mediate postsynaptic but not presynaptic transmitter actions in hippocampal neurons. *Neuron* **19**, 687–695.

Luscher C & Slesinger PA (2010). Emerging roles for G protein-gated inwardly rectifying potassium (GIRK) channels in health and disease. *Nat Rev Neurosci* **11**, 301–315.

Maywood ES, Okamura H & Hastings MH (2002). Opposing actions of neuropeptide Y and light on the expression of circadian clock genes in the mouse suprachiasmatic nuclei. *Eur J Neurosci* **15**, 216–220.

Mistlberger RE & Skene DJ (2005). Nonphotic entrainment in humans? *J Biol Rhythms* **20**, 339–352.

Nelson CS, Marino JL & Allen CN (1996). Melatonin receptors activate heteromeric G-protein coupled Kir3 channels. *Neuroreport* **7**, 717–720.

Paredes MF, Greenwood J & Baraban SC (2003). Neuropeptide Y modulates a G protein-coupled inwardly rectifying potassium current in the mouse hippocampus. *Neurosci Lett* **340**, 9–12.

Pickard GE (1994). Intergeniculate leaflet ablation alters circadian rhythms in the mouse. *Neuroreport* **5**, 2186–2188.

Pickard GE, Ralph MR & Menaker M (1987). The intergeniculate leaflet partially mediates effects of light on circadian rhythms. *J Biol Rhythms* **2**, 35–56.

Pizarro A, Hayer K, Lahens NF & Hogenesch JB (2013). CircaDB: a database of mammalian circadian gene expression profiles. *Nucleic Acids Res* **41**, D1009–1013.

Ruiz de Elvira MC, Persaud R & Coen CW (1992). Use of running wheels regulates the effects of the ovaries on circadian rhythms. *Physiol Behav* **52**, 277–284.

Schaap J, Bos NP, de Jeu MT, Geurtsen AM, Meijer JH & Pennartz CM (1999). Neurons of the rat suprachiasmatic nucleus show a circadian rhythm in membrane properties that is lost during prolonged whole-cell recording. *Brain Res* **815**, 154–166.

Scott FF, Belle MD, Delagrange P & Piggins HD (2010). Electrophysiological effects of melatonin on mouse Per1 and non-Per1 suprachiasmatic nuclei neurones *in vitro*. *J Neuroendocrinol* **22**, 1148–1156.

Shusterman V, Warman E, London B & Schwartzman D (2012). Nocturnal peak in atrial tachyarrhythmia occurrence as a function of arrhythmia burden. *J Cardiovasc Electrophysiol* **23**, 604–611.

Signorini S, Liao YJ, Duncan SA, Jan LY & Stoffel M (1997). Normal cerebellar development but susceptibility to seizures in mice lacking G protein-coupled, inwardly rectifying K$^+$ channel GIRK2. *Proc Natl Acad Sci U S A* **94**, 923–927.

Soscia SJ & Harrington ME (2004). Neuropeptide Y attenuates NMDA-induced phase shifts in the SCN of NPY Y1 receptor knockout mice *in vitro*. *Brain Res* **1023**, 148–153.

Soscia SJ & Harrington ME (2005). Neuropeptide Y does not reset the circadian clock in NPY Y2–/– mice. *Neurosci Lett* **373**, 175–178.

Takigawa M, Kawamura M, Noda T, Yamada Y, Miyamoto K, Okamura H, Satomi K, Aiba T, Kamakura S, Sakaguchi T, Mizusawa Y, Itoh H, Horie M & Shimizu W. (2012). Seasonal and circadian distributions of cardiac events in genotyped patients with congenital long QT syndrome. *Circ J* **76**, 2112–2118.

Turek FW, Penev P, Zhang Y, van Reeth O & Zee P (1995). Effects of age on the circadian system. *Neurosci Biobehav Rev* **19**, 53–58.

van den Pol AN, Obrietan K, Chen G & Belousov AB (1996). Neuropeptide Y-mediated long-term depression of excitatory activity in suprachiasmatic nucleus neurons. *J Neurosci* **16**, 5883–5895.

Vyazovskiy VV, Kopp C, Wigger E, Jones ME, Simpson ER & Tobler I (2006). Sleep and rest regulation in young and old oestrogen-deficient female mice. *J Neuroendocrinol* **18**, 567–576.

Wang TA, Yu YV, Govindaiah G, Ye X, Artinian L, Coleman TP, Sweedler JV, Cox CL & Gillette MU (2012). Circadian rhythm of redox state regulates excitability in suprachiasmatic nucleus neurons. *Science* **337**, 839–842.

Wang Z (2013). miRNA in the regulation of ion channel/transporter expression. *Compr Physiol* **3**, 599–653.

Welsh DK, Takahashi JS & Kay SA (2010). Suprachiasmatic nucleus: cell autonomy and network properties. *Annu Rev Physiol* **72**, 551–577.

Wydeven N, Marron Fernandez de Velasco E, Du Y, Benneyworth MA, Hearing MC, Fischer RA, Thomas MJ, Weaver CD & Wickman K (2014). Mechanisms underlying the activation of G-protein-gated inwardly rectifying K$^+$ (GIRK) channels by the novel anxiolytic drug, ML297. *Proc Natl Acad Sci U S A* **111**, 10755–10760.

Yannielli PC, Brewer JM & Harrington ME (2004). Blockade of the NPY Y5 receptor potentiates circadian responses to light: complementary *in vivo* and *in vitro* studies. *Eur J Neurosci* **19**, 891–897.

Yannielli P & Harrington ME (2004). Let there be 'more' light: enhancement of light actions on the circadian system. *Prog Neurobiol* **74**, 59–76.

Yannielli PC & Harrington ME (2000). Neuropeptide Y applied *in vitro* can block the phase shifts induced by light *in vivo*. *Neuroreport* **11**, 1587–1591.

Yoo SH, Yamazaki S, Lowrey PL, Shimomura K, Ko CH, Buhr ED, Siepka SM, Hong HK, Oh WJ, Yoo OJ, Menaker M & Takahashi JS (2004). PERIOD2::LUCIFERASE real-time reporting of circadian dynamics reveals persistent. *Proc Natl Acad Sci U S A* **101**, 5339–5346.

Zarowski M, Loddenkemper T, Vendrame M, Alexopoulos AV, Wyllie E & Kothare SV (2011). Circadian distribution and sleep/wake patterns of generalized seizures in children. *Epilepsia* **52**, 1076–1083.

Zuberi Z, Birnbaumer L & Tinker A (2008). The role of inhibitory heterotrimeric G proteins in the control of *in vivo* heart rate dynamics. *Am J Physiol Regul Integr Comp Physiol* **295**, R1822–R1830.

Additional information

Competing interests

No authors have any conflicts of interest.

Author contributions

L.M.H. and K.L.G. were responsible for conception and design of the experiments, collection, analysis and interpretation of the data, and drafting the article. H.E.M., J.R.P. and R.L.J. contributed to collection, analysis, and interpretation of the data. All authors read and approved the final version of the manuscript.